Class A GPCRs harness the energy of membrane potential to increase their sensitivity and selectivity

Daria N. Shalaeva[1,2], **Dmitry A. Cherepanov**[2,4], **Michael Y. Galperin**[5], **Gert Vriend**[6], **Armen Y. Mulkidjanian**[1,2,3,*]

[1]School of Physics, Osnabrueck University, 49069, Osnabrück, Germany; [2]A.N. Belozersky Institute of Physico-Chemical Biology, Lomonosov Moscow State University, Moscow 117999, Russia; [3]School of Bioengineering and Bioinformatics, Lomonosov Moscow State University, Moscow 117999, Russia; [4]N.N. Semenov Institute of Chemical Physics, Russian Academy of Sciences, 119991 Moscow, Russia; [5]National Center for Biotechnology Information, National Library of Medicine, National Institutes of Health, Bethesda, Maryland 20894, USA; [6]Centre for Molecular and Biomolecular Informatics, Radboud University Medical Centre, 6525 HP Nijmegen, The Netherlands

Abstract

The human genome contains about 700 genes of G protein-coupled receptors (GPCRs) of class A; these seven-helical membrane proteins are the targets of almost half of all known drugs. In the middle of the helix bundle, crystal structures revealed a highly conserved sodium-binding site, which is connected with the extracellular side by a water-filled tunnel. This binding site contains a sodium ion in GPCRs crystallized in their inactive conformations, but not in GPCRs that were trapped in agonist-bound active conformations. The escape route of the sodium ion upon the inactive-to-active transition and its very direction, either into the cytoplasm or back outside the cell, have remained obscure. By modeling the available experimental data we show that the sodium gradient over the cell membrane would increase the sensitivity of GPCRs if their activation were thermodynamically coupled to the sodium ion translocation into the cytoplasm, but decrease it if the sodium ion retreats into the extracellular space upon receptor activation. The model quantitatively describes the available data on both activation and suppression of distinct GPCRs by membrane voltage. The model also predicts selective amplification of the signal from (endogenous) agonists if only they, but not their (partial) analogs, could induce sodium translocation. Comparative structure and sequence analyses of sodium-binding GPCRs indicate a

key role for the conserved leucine residue in the second transmembrane helix (Leu2.46) in coupling sodium translocation to receptor activation. Hence, class A GPCRs appear to harness the energy of the transmembrane sodium potential to increase their sensitivity and selectivity.

Keywords

G protein-coupled receptors; receptor activation; sodium transport; agonist binding; cell signaling; adrenoreceptor; muscarinic receptor; membrane potential

1.   Introduction

G-protein coupled receptors (GPCRs) are integral membrane proteins that consist of seven transmembrane (TM) helices surrounding a relatively polar core [1–3], see Fig. 1A–C. In most GPCRs, binding of an endogenous ligand (agonist) by an "inactive" form of protein causes a conformational change of the helical bundle (Fig. 1). The activated GPCR interacts with a G protein, which then triggers the intracellular signaling cascade. GPCRs are widespread among eukaryotes and are intensively studied for their ability to regulate various cellular processes. Human GPCRs serve as targets for about half of all known drugs [1].

GPCRs are divided into several classes: rhodopsin-like receptors (class A), secretin receptors (class B), glutamate receptors (class C), fungal mating pheromone receptors (class D), cAMP receptors (class E), and frizzled receptors (class F). Sequence and structure comparisons of GPCRs support the notion that most, if not all, of them have a common evolutionary origin [4, 5]. Different classes of GPCRs are unevenly represented in sequenced genomes from various eukaryotic lineages. In humans, class A GPCRs are the largest protein family with about 700 genes, whereas all other classes of GPCRs together have only about 150 representatives [4].

The recent avalanche of high-resolution X-ray structures of GPCRs in ligand-free, agonist-bound, and antagonist-bound forms revealed many important features of their functioning, see [1–3, 6–15] and references therein. The major feature is that activation of GPCRs is associated with a large displacement of the cytoplasmic half of helix 6. A conserved Trp residue in the middle of this helix (Trp6.48 according to the Ballesteros–Weinstein numeration for class A GPCRs as modified by Isberg et al. [16, 17], used hereafter) serves as the pivot of this motion, see Fig. 1C and [2, 7, 18–24]. Another feature uncovered by these structures was the presence of Na^+ ions in the vicinity of the ligand-binding sites in several class A GPCRs, see [10, 13, 14, 25–27] and references therein. The Na^+ binding site is connected to the extracellular side through a clearly visible tunnel, but separated from the cytoplasmic side by a cluster of hydrophobic residues (Fig. 1A, B and [24, 25]). The Na^+ binding residues are highly conserved among class A GPCRs [25, 27], indicating that the Na^+ ion must be functionally important. Indeed, replacement of the key Na^+-binding Asp2.50 residue in helix 2 (see Fig. 1) facilitates binding of agonists by increasing the association constants by 2–3 orders of magnitude in many, albeit not all, cases, see [25, 27–32] and references therein. In many cases, Na^+ depletion increased the basal activity of the respective receptor in the absence of an agonist, suggesting that the Na^+ ion stabilizes the inactive state of the receptor [25, 27–33] and references therein. This interpretation is

consistent with the structural data that show that the Na^+ ion is not observed in GPCRs in an active conformation (bound with agonists); the Na^+-binding pocket collapses from ~200 to 70 $Å^3$ due to the movements of TM helices upon activation, see Fig. 1, [10, 11, 25, 27, 34, 35] and references therein. The absence of a space for the Na^+ ion suggests that it leaves the receptor upon activation.

Several years ago, Katritch and colleagues made a seminal suggestion that the Na^+ ion does not return into the extracellular medium but instead gets released into the cytoplasm upon GPCR activation [25]. The suggested mechanism, however, would require a transient opening of a conduit for the Na^+ ion. The available structures of activated, Na^+-lacking GPCRs show no such a conduit, see Fig. 1 [11, 34, 35] and references therein. Still, several computer simulations indicated a possibility of a transient water-filled channel connecting the Na^+-binding site with the cytoplasm [23, 32, 36, 37]. The proposed ability for the Na^+ ion to traverse the GPCR molecule is also supported by the structural similarity between GPCRs and Na^+-translocating bacterial rhodopsins (see Fig. S1 and [38–40] for structures), which suggests their common origin [5] and a common ability to translocate Na^+ ions.

Since the cytoplasm is negatively charged relatively to the extracellular medium, transfer of a Na^+ cation into the cell could give an energy boost for the GPCR activation [25]. Depolarization of the membrane would thus prevent the GPCR activation. This kind of behavior has been, indeed, observed with many GPCRs. Still, some GPCRs, by contrast, were activated by depolarization, whereas some others were insensitive to it; see [41, 42] for reviews and Table S1 for further references. Hence, the relation between the transmembrane gradient of sodium ions and GPCR activation deserves further clarification.

Unfortunately, the anticipated translocation of only one Na^+ ion per activation event translates into a very weak electric current, which hampers the experimental tracking of this process. In the absence of direct experimental data on the Na^+ ion translocation, we have addressed it through modeling and comparative structural analyses.

Here, building on our previous study that described the similarity of GPCRs with Na^+-translocating microbial rhodopsins [5], we modeled class A GPCRs as facultative sodium carriers. The model implies that the bound Na^+ ion, upon activation, can either slip into the cytoplasm via a transiently opened passage (the carrier-on mode of operation) or return to the extracellular side (the carrier-off mode of operation). Just by varying the dissociation constants for the agonist and the sodium ion, our model quantitatively describes the available data on both activation and suppression of GPCRs by membrane voltage. In addition, by combining evolutionary analyses with structural comparisons of GPCRs, we have identified the strictly conserved leucine residue in the second transmembrane helix (Leu2.46 in class A GPCRs) as the key player in coupling sodium translocation to receptor activation.

In summary, this study proposes a mechanism that links the activation of class A GPCRs, via electrogenic Na^+ translocation, with the energy of membrane potential. The ability to harness the energy of membrane potential offers an explanation for the high sensitivity and selectivity of class A GPCRs and for their abundance in eukaryotes.

2. Methods

2.1. Construction and solution of the model of Na⁺ -coupled GPCR activation.

Here we present the solution of the model of GPCR activation (Fig. 2A, B). The physical meanings of parameters used and their estimates are considered in the Results. The model includes three binary transitions: (i) activation of the receptor, (ii) binding of the Na⁺ ion, and (iii) binding of a signaling molecule (e.g. an agonist). Each of these transitions is characterized by its equilibrium constant: the receptor activation constant L, the Na⁺ association constant M, and the agonist association constant N. These three transitions can be presented as a cubic graph with 8 separate states numbered from 1 to 8 (Fig. 2B, Table 1). The allosteric coefficients α, β, γ, and δ describe the extent of coupling between the transitions, i.e. their interdependence. The model implies two possible operation modes differing in the Na⁺ ion behavior upon the receptor activation: in the carrier-on mode 1, the cation barges through the membrane into the cytoplasm, while in the carrier-off mode 2 the cation returns into the extracellular space.

Here, Φ_1 and Φ_2 are the probabilistic Boltzmann-like electrostatic terms of Na⁺ ion translocation, which are equal to

$$\Phi_1 = \exp\left[\theta \cdot e \cdot \Delta\psi / k_B T\right] \tag{1}$$

and

$$\Phi_2 = \exp\left[(\theta - 1) \cdot e \cdot \Delta\psi / k_B T\right] \tag{2}$$

where ψ is the transmembrane electric potential, e is the elementary charge, k_B is the Boltzmann constant, T is the temperature, and the coefficient θ reflects the depth of the Na⁺-binding site in the membrane, with θ=0 corresponding to the Na⁺ ion on the extracellular side of the membrane and θ=1 corresponding to the Na⁺ ion on the cytoplasmic side of the membrane.

In total, the system includes 12 elementary transitions, which correspond to the cube edges in Fig. 2B. The transitions between the inactive (R) and active (R*) states of the receptor are assumed to be the slowest in the system.

In the carrier-off mode, the enzyme is assumed to be in thermodynamic equilibrium, i.e. all forward and backward transitions are equal to each other, so the principle of detailed balance is applied to all inactive and active receptor states. The probabilities P_1, …, P_8 are defined by the respective equilibrium constants (Table 1, right column) and could be calculated directly by the normalization requirement:

$$\sum_{i = 1..8} P_i = 1$$

In the carrier-on mode, the principle of detailed balance could be applied separately to all inactive (blue arrows in Fig. 2B) and all active (red arrows in Fig. 2B) receptor states, whereas the transitions between active and inactive states (green arrows in Fig. 2B) were

treated as nonequilibrium transitions. By this reason, we considered explicitly only the rate constants k_{nm} of the four forward transitions $n{\rightarrow}m$ between the inactive states n and the active states m, and the rate constants k_{mn} of the corresponding backward transitions $m{\rightarrow}n$. All the other transitions were assumed to be in thermodynamic equilibrium and defined by respective equilibrium constants (Table 1, left column).

In the stationary state of enzyme operation in the carrier-on mode, the probabilities P_1, …, P_8 can be found as follows. The cumulative forward and backward transition probabilities between all active and inactive states match each other:

$$k_{15}P_1 + k_{26}P_2 + k_{37}P_3 + k_{48}P_4 = k_{51}P_5 + k_{62}P_6 + k_{73}P_7 + k_{84}P_8, \qquad (3)$$

where probabilities P_{1-4} correspond to the respective inactive states, and P_{5-8} – to the respective active states, whereas k_{nm} and k_{mn} are the respective transition rate constants. The transition rate constants are not independent, they satisfy the thermodynamic relationship $k_{forward} / k_{back} = e^{-\ G/RT}$, so the Eq. (3) can be rewritten as following:

$$k_{15}[P_1 + \alpha^{1/2}P_2 + \beta^{1/2}P_3 + (\alpha\beta\delta)^{1/2}P_4] = k_{51}[P_5 + \alpha^{-1/2}P_6 + \beta^{-1/2}P_7 + (\alpha\beta\delta)^{-1/2}P_8]$$

The membrane potential affects the cation translocation by changing the equilibrium constants of Na^+ binding, both in inactive (Φ_1) and active (Φ_2) states. This leads to the relation:

$$P_5 = \xi \cdot L \cdot P_1,$$

where

$$L = k_{15}/k_{51}$$

and

$$\xi = \frac{1 + \alpha^{1/2}\Phi_1 X_{out} + \beta^{1/2}Y + (\alpha\beta\delta)^{1/2}\Phi_1\gamma X_{out}Y}{1 + \alpha^{1/2}\Phi_2 X_{in} + \beta^{1/2}Y + (\alpha\beta\delta)^{1/2}\Phi_2\gamma X_{in}Y},$$

where $X_{in}{=}M[Na^+]_{in}$, $X_{out}{=}M[Na^+]_{out}$, and $Y{=}N[agonist]$, respectively. To these equations we must add the probabilities normalization requirement:

$$\sum_{i\,=\,1..8} P_i = 1$$

The resulting set of equations provides a solution to the model.

Suggested models for GPCR activation were implemented as Matlab R2017a functions (Mathworks, Inc.) [43]. Experimental data were obtained from respective publications and

were fitted with model functions using the Matlab's "lsqcurvefit" function. During the fit, the allosteric coefficients α-δ and the depth of the Na^+-binding site were kept constant. The goal was to find coefficients M (Na^+-binding constant) and N (agonist-binding constant) that provided the best fit of the experimental data (two sets of data points obtained at different membrane potential) with the two model curves calculated with identical parameters except for the membrane potential values.

2.2. Structure analysis

Structure superposition and visualization were performed with PyMol v 1.7 (Schrödinger LLC) [44] and YASARA [45]. Structure analyses were performed with the WHAT IF [46] subset of the YASARA Twinset. Cavities and caves were calculated using the method by Voorintholt et al [47] with a spherical probe of the 1.4 Å radius. These were visualized using a 1 Å resolution grid. Structures were superposed using the method of Vriend and Sander [48]. Rotamer distributions were calculated using the method of Chinea et al. [49]. Briefly, the rotamer distribution software searches the PDB for stretches of five residues that (i) have a very similar backbone as observed in the local structure and (ii) have the same middle residue as the local structure. The obtained database stretches are then superposed on the local structure, but only the side chain of the middle residue is shown.

3. Results

3.1. Modeling Na^+ translocation in GPCRs

We developed a model of GPCR activation that is analogous to earlier approaches to modeling GPCRs [50–53] but, as in case of energy-converting membrane proteins [54], takes into account the possibility of electrogenic (i.e. coupled to the transmembrane potential) translocation of a single Na^+ ion by a GPCR concomitantly with its activation. Here we describe the physical meaning of the parameters and provide their initial values. The solution of the model is described in Methods.

The model considers a GPCR ensemble large enough for thermodynamic modeling. Each receptor exists in a steady state balance between its active and inactive states; agonists shift the distribution towards the active states, whereas Na^+ binding stabilizes the inactive states (Fig. 2A). Both the active and inactive states were shown to exist as series of fast exchanging conformational sub-states [2, 55–57]; for simplicity, we do not consider these sub-states in the model. Also for simplicity, it is just assumed that an activated GPCR triggers the signaling cascade; the interaction of the active state with any other component (G-protein or arrestin) is not modeled. The model includes three binary transitions: (i) activation of the receptor, (ii) binding of the Na^+ ion, and (iii) binding of a signaling molecule (e.g. an agonist). These three transitions can be presented as a cubic graph with 8 separate states (Fig. 2B). Each of the transitions is determined by its equilibrium constant: the receptor activation constant L, the Na^+ association constant M, and the agonist association constant N (Table 2).

As shown in Fig. 2A, a GPCR has two operation modes: in the carrier-on mode (mode 1), the Na^+-binding site can communicate with the cytoplasm, whereas in the carrier-off mode

(mode 2), the Na^+-binding site communicates only with the extracellular side. If the receptor operates in the carrier-off mode, all its eight states are in a thermodynamic equilibrium, and we can apply to them the principle of detailed balance (the forward and backward rates of transitions match each other). If the GPCR can translocate a Na^+ ion across the membrane (carrier-on mode), then, under the conditions of a non-zero transmembrane electrochemical Na^+ potential difference (Na^+ gradient), the slowest transitions in Fig. 1B are not in equilibrium (the forward and backward rates of these transitions do not match each other). However, since the activation of the receptor is much slower than any other transitions in the model, the detailed balance principle can be applied separately to all inactive and all active receptor states (the left-hand and right-hand sides of the cubic diagram in Fig. 2B, respectively, see also Methods).

Our model assumes that the rate-limiting step is the slow "activating" conformational transition [53]. The agonist binding to the initial encounter state R, binding/release of the Na^+ ion, and conformational transitions within inactive and active states are considered rapid as compared to the activating R to R* transition, which appears to be coupled with the pivotal movement of helix 6 in most class A GPCRs [2, 7, 18–24]. In the case of opsin, the pivotal movement occurred slower than at 10^{-4} s with the activation energy as high as 60 kJ/mol [19, 58]. The slowness of the transition was also confirmed by NMR data [21, 56]. The assumption of the slow activating transition is in agreement with both the induced-fit model [52, 53, 57] and the conformational selection model [56]; these two models appear to describe the operation of most GPCRs.

In the absence of an agonist, the fraction of receptors in the R* state is determined by the equilibrium constant L. Generally, L should be about 1, otherwise the receptor will be blocked in one of the two states. The exact value of L, however, is unknown; its determination requires experimental data on the distribution of active and inactive states in the absence of both Na^+ ions and agonists (ligands), which are difficult to obtain. In this study, we set the value L=1. This value was chosen to produce very little activity in the presence of Na^+ ions, but also to exhibit some activity in their absence, since this would most closely mimic the behavior of experimental systems, see [25, 26, 28, 30–32] and references therein. Specifically, β_2-adrenergic receptors were biased towards inactive conformation both when studied by ^{19}F-NMR and double electron-electron resonance spectroscopy (detergent-stabilized samples, 100 mM NaCl) [2] and by single-molecule monitoring of fluorescent probes (nanodisc-embedded receptors, 150 mM NaCl) [55].

The initial values of the agonist and sodium association constants were set to N=10^7 M^{-1} and M=10^3 M^{-1}, respectively, in accordance with the physiologically relevant agonist and sodium concentrations, see [26, 59, 60] and references therein.

The allosteric coefficients α, β, γ, and δ describe the extent of coupling between the transitions, i.e. their interdependence, see Table 2. The coefficient α reflects the effect of Na^+ ion binding on the receptor activation. Based on experimental evidence, Na^+ ions inhibit receptor activation [25, 27–32], thus this coefficient should be $\ll 1$. The coefficient β reflects the effect of agonist binding on the activation of the receptor. As agonist binding stimulates receptor activation, this value was expected to be $\gg 1$. The coefficient γ reflects

the effect of agonist binding on the Na^+ ion binding. Available crystal structures of GPCR with Na^+ ion bound usually do not contain an agonist molecule, whereas the structures of the same proteins with agonist bound have no space for a Na^+ ion [25]; therefore, the value of γ was expected to be $\ll 1$. The triple allosteric interaction coefficient δ reflects the coupling between all three processes. Probabilities of individual states are also affected by Na^+ concentrations, which were set at physiological values of $[Na]_{out} = 140$ mM and $[Na]_{in} = 10$ mM (Table 2).

Fig. S2 shows how the shape of activation curves varies with variation of parameters α, β, γ, and δ in the carrier-on mode. These concentration-response curves report the sensitivity of the receptor: they show how much agonist is needed to activate the receptor. Fig. S2 shows that increasing the value of δ, which characterizes the coupling between the (i) binding of agonist, (ii) release of the Na^+ ion into the cytoplasm and (iii) activation of the receptor, increases the sensitivity of the receptor (less agonist is needed for activation, see Fig. S2D).

Based on comparison of the fit curves (Fig. S2) with experimentally measured typical activation curves for several GPCRs, we set the initial values of α, β, and γ to 1000, 0.001, and 0.01, respectively (Table 2). Then the product $\alpha\beta\gamma$ equals 0.01, which means that the concurrent binding of the Na^+ ion and agonist shifts the receptor into the inactive state. Such an inactivation could be avoided by setting δ, the triple allosteric interaction coefficient that reflects the coupling between all three processes, at $\gg 1$. The value of δ was initially set to 100, so that the product of multiplication of all coefficients was 1.

Because of the charge of the Na^+ ion, the probabilities of states in Fig. 2B would also be affected by membrane voltage. Since cell cytoplasm is charged negatively relative to the extracellular medium, membrane voltage pushes the Na^+ ion from the extracellular side to the cytoplasmic side of the membrane. Hence, membrane voltage favors the translocation of the Na^+ ion (i) from the outside into the Na^+-binding site and (ii) from the Na^+-binding site into the cytoplasm. In contrast, the retreat of the Na^+ ion to the extracellular site would be hampered by membrane voltage. The respective probabilistic Boltzmann-like electrostatic terms of Na^+ ion translocation are given by Equations (1) and (2), respectively, in Methods. Both these terms contain the coefficient θ that reflects the depth of the Na^+-binding site in the membrane, with $\theta = 0$ corresponding to the Na^+ ion on the extracellular side of the membrane and $\theta = 1$ corresponding to the Na^+ ion on the cytoplasmic side of the membrane. Based on the actual position of the Na^+ ion in available crystal structures (Fig. 1) and assuming a symmetrical distribution of dielectric permittivity value along the transmembrane axis, we have set $\theta = 0.65$ as an initial value for the Na^+-binding site in class A GPCRs.

As shown in Fig. 2C and 2D, the same initial parameters from Table 2 yielded different activation curves and different dependence on the membrane voltage depending on the operation mode. In the carrier-on mode, the receptor displays the highest sensitivity at the membrane voltage of -200 mV, while neutral and positive voltage values lead to weaker activation, with more agonist required to reach the same activation level. In the carrier-off mode, the dependence of activation on the membrane voltage is opposite: the receptor is

more efficient at positive voltage values; in this mode, the sensitivity of concentration-response curves to the voltage is much less than in the carrier-on mode.

The curves in Fig. 2C, D and Fig. S2 were calculated at fixed physiological concentrations of Na^+ ions in the external medium and in the cytoplasm (Table 2). In Fig. 2, panels E and F show the activation curves as a function of external Na^+ concentration. Decreasing the Na^+ levels increases both the sensitivity of the receptor and the probability of receptor activation in the absence of agonists, in agreement with experimental observations [25, 27–32] and references therein.

3.2. Comparison with experimental data

Several studies have reported voltage-dependent signaling in different GPCRs, see Table S1 and [41, 42] for reviews. The membrane voltage of physiological sideness (with cytoplasmic side negatively charged) usually activated GPCRs, although in some cases, e.g. in the muscarinic acetylcholine receptor M_1, membrane voltage decreased the activity of the receptor [59, 61, 62]. In early studies of voltage-dependent behavior of GPCRs, their activation was followed via downstream reactions, e.g. by measuring the conductance of the GPCR-regulated ion channels, see Table S1, [41, 42] and references therein. However, the potential voltage-dependence of the channels themselves could make the data interpretation ambiguous. Therefore we limited our scope to the data on voltage dependence of GPCR activation as obtained by using FRET-based biosensors [34, 59, 60]. These sensors responded to the outward movement of the transmembrane helix 6 which was directly linked to receptor activation [2, 7, 18–24]. Using this technique, Rinne and colleagues showed that membrane voltage increased the sensitivity of the α_{2A} adrenoreceptor to norepinephrine [60]. In addition, membrane voltage increased the sensitivity of muscarinic acetylcholine receptors M_3 and M_5 to their full agonists acetylcholine and carbachol, but decreased the sensitivity to the same full agonists in the case of the muscarinic acetylcholine receptor M_1 [59].

We tested whether our model could describe the data of Rinne and colleagues [59, 60]. To perform the fitting, experimental data points were extracted from the respective publications. In each case, fits were separately performed for the carrier-on and carrier-off modes, respectively. For each mode, two sets of data points (as measured at two voltage values, e.g. -90 and +60 mV) were fitted. The two fit curves were calculated by using the same parameter sets (see Table 2), with the only difference being the voltage values that were taken from respective experimental data. Both curves were fitted simultaneously by varying only two parameters, namely the Na^+ binding constant M and agonist binding constant N, which were kept the same for both voltage values in each case. All other parameters were as in Table 2. In addition, we performed separate fits with $\beta=100$, see Table 3.

The fit curves are shown in Fig. 3 and the fit parameters are listed in Table 3. In each case, only one of the two tested modes provided a good fit. In cases where the membrane voltage increased the sensitivity of the receptor, the experimental data could be fit by the carrier-on model. For the data in Fig. 3C, where the sensitivity was decreased by membrane voltage, the carrier-off mode provided a good fit. Varying the θ value, which was initially determined from structure analysis, did not lead to notable fit improvements (data not shown). It is

noteworthy that the agonist association constants in Table 3 correspond to the so-called intrinsic association constants (K_a), which could be much smaller than the observable association constants (K_{obs}), see [53, 63].

By using essentially the same set of parameters from Table 2 and varying only the values M and N, it was possible to quantitatively fit also the previously obtained experimental data on the influence of membrane voltage on the activation of GPCRs as traced via downstream reactions (Table S1). An example of such a fit is presented in Fig. S3.

Our modeling of experimental data speaks against the obligatory coupling between the activation of a GPCR and transmembrane translocation of a Na^+ ion into the cytoplasm. It appears that in some GPCRs, the Na^+ ion could retract, upon activation, into the extracellular medium. In most studied cases, however, the experimental data were better described by the carrier-on operation mode where binding of an agonist was mechanistically coupled to the voltage-driven translocation of the Na^+ ion into the cytoplasm.

4. Discussion

4.1. Modeling the behavior of GPCRs

Here, staying in the traditional bioenergetics framework, we considered Na^+-dependent GPCRs as potential electrogenic Na^+ carriers. The ability of GPCRs to provide a passage for a Na^+ ion follows from (i) the results of molecular dynamics simulations [23, 31, 32, 36, 37], (i) the evolutionary relatedness of GPCRs to, and structural similarity with such dedicated transporters as Na^+-dependent bacterial rhodopsin (NR) and channelrhodopsin (see see the discussion in subsection 4.3, Figs. S1, S5 and [5]); and (iii) the data on so-called "gating currents" or "sensory currents", measured in response to imposed membrane voltage with some GPCRs (see [62, 64] and references therein), which, according to Vickery and colleagues may reflect the movement of a Na^+ ion from its binding site into the cytoplasm [42].

To clarify the benefits from Na^+ translocation, let us consider the thermodynamics of a membrane receptor. An "ultimately sensitive" receptor should stay inactive in the absence of agonists and get activated (e.g. by changing its conformation from R to R*) in response to the very first arriving molecule(s) of agonist. In such a system, the free energy needed to drive the conformational change is provided by the binding of agonist; the amount of this free energy is, however, small when the concentration of agonist is comparable with its dissociation constant. Indeed, the free energy of binding can be determined as

$$\Delta G \quad = RTln\frac{Kd}{[L]}$$

where Kd is the dissociation constant of the ligand (e.g. agonist) and $[L]$ is the concentration of the ligand. Then, if the dissociation constant of an agonist is 10^{-7} M, the free energy of its binding will be zero at 10^{-7} M of agonist and only -6 kJ/mol at 10^{-6} M of agonist. With such a small energy input, the activation would be possible only if the equilibrium constant between R and R* is small (i.e. close to unity, as in our modeling). Then, however, because

the energy of thermal fluctuations is 2.5 kJ/mol (one RT) at room temperature, 10% of receptors would stay constantly activated even in the absence of agonist and would produce spurious noisy signal.

Selective stabilization of receptors in their inactive state by Na^+ ions, which are abundant outside the cell, would help to silence the intrinsically noisy GPCRs in the absence of agonist molecules. However, such a noise reduction would decrease the sensitivity of GPCRs. To activate a Na^+-blocked receptor, proportionally higher levels of agonists would be needed. This conundrum can be solved only by invoking an external source of free energy and coupling it to the receptor activation. The data on voltage dependence of some GPCRs in Fig. 3A,B and S3 indicate that these GPCRs showed higher sensitivity in the presence of the transmembrane electric field, which indicates their ability to use the energy of this field. At physiological membrane voltage of about −100 mV, the strength of the electric field that pushes the Na^+ ion across the membrane is approx. 10^7 V/m. The energy of this field could be, however, used only if the receptor activation is mechanistically coupled to the displacement of the ion.

How much free energy could be gained this way *in vivo*? In experiments where the voltage was varied by 150 mV (between −90 mV and 60 mV, see Fig. 3, S3), only the membrane voltage, but not the Na^+ concentrations, were varied. *In vivo*, the movement of the Na^+ ion would be driven both by the voltage on the cellular membrane ψ (~−100 mV) and concentration difference of Na^+ (140 mM outside *versus* < 10 mM inside). By analogy with the proton-motive force introduced by Mitchell for describing the proton-motive energy conversion [65], the corresponding sodium-motive force (*smf*), in the case of Na^+-translocating membrane enzymes, could be defined as

$$smf \quad = \; -\Delta\psi + \frac{2.3RT}{F}lg\frac{\left[Na^+\right]_{out}}{\left[Na^+\right]_{in}} = \; -\Delta\psi + \frac{2.3RT}{F}\Delta pNa,$$

where 2.3RT/F is 59.1 mV at 298°K [66].

In case of GPCRs, the value of *smf* would depend on the extent of the coupled transmembrane charge transfer. After the escape of the Na^+ ion into the cytoplasm, the Asp2.50 residue is unlikely to stay deprotonated and negatively charged in the middle of the membrane, it would rather accept a proton from the external medium [37]. The corresponding displacement of a proton would be driven by membrane voltage; it, however, could be either coupled to the activation of the receptor or not. If the proton displacement is uncoupled (e.g. because protonation of Asp2.50 is slow and happens after the activation of the GPCR), the amount of free energy derived from the Na^+ translocation could be estimated as $(\sim -\Delta\psi(1-\theta) + \frac{2.3RT}{F}\Delta pNa)$ or ~ 120 meV. As it follows from Fig. 2C, the *smf* of 120 meV, at δ >> 1.0, would increase the receptor sensitivity up to an order of magnitude. If the reprotonation of Asp2.50 is coupled to the activation, as argued by Vickery and colleagues [37], the respective *smf* of ~ 170 mV $(\sim -\Delta\psi + \frac{2.3RT}{F}\Delta pNa)$ could increase the sensitivity by almost two orders of magnitude (see Fig. 2C). Furthermore, reprotonation of Asp2.50 could

be productive in some GPCRs and futile in other GPCRs contributing to the variations of voltage effects, as reviewed in [37, 42].

Our modeling of experimental data (Fig. 3 and S3) supports the idea that Na^+-translocating GPCRs, when operating in the carrier-on mode, could use the energy of the transmembrane electric field to amplify the signal. Devices that use the energy of an external electric field to amplify a weak signal are called field effect transistors.

Additionally, the same electric field, by preventing the escape of the bound Na^+ ion to the extracellular side and stabilizing the inactive GPCR conformation, would decrease the noise in the absence of agonist. Hence, Na^+-dependent GPCRs can work as electrochemical field effect transistors in which the electric field is additionally used to suppress the noise.

There are even more benefits from coupling the translocation of the Na^+ ion with receptor activation. Since the equilibrium constant between the active and inactive states of GPCRs is low (Table 2), the equilibrium, in principle, could be shifted towards the active state in multiple ways in response to binding of various ligands to different patches in the ligand-binding pocket. The above-described amplification mechanism, however, would be involved only when the binding of an agonist molecule would prevent the retreat of the Na^+ ion into the extracellular media upon activation [25]. The Na^+ binding site is connected with the extracellular space by a polar cavity (Fig. 1A, B), so that the retreat of a Na^+ ion through this cavity upon activation is mechanistically easier than its corkscrewing in the opposite direction through the layer of hydrophobic residues - unless the agonist binds in such a specific way that the retreat of the Na^+ ion is blocked and it is forced to escape in the opposite direction. Apparently, only some specific modes of agonist binding would prevent the retreat of the Na^+ ion and thus enable the coupling between its electrogenic translocation into the cell and the receptor activation. The signal of such agonist molecules would be amplified by electric field (carrier-on mode), whereas the signal of other, e.g. partial agonists would be weakened by the field (carrier-off mode), which would dramatically increase the chemical selectivity of the receptor.

It could be anticipated that the endogenous agonists of studied GPCRs should be among those effectors whose signals are amplified by membrane voltage. Indeed, in the muscarinic acetylcholine receptor M_2, the membrane voltage potentiated the signal from the endogenous full agonist acetylcholine, but decreased the signal from the drug pilocarpine, a partial agonist, see Fig. S3, [67, 68] and Table S1 for further references. Additionally, the voltage sensitivity of the M_2 receptor was shown to be altered by mutations in the orthosteric ligand-binding site, indicating a direct connection between the agonist binding and voltage effects [67].

In the case of the muscarinic acetylcholine receptor M_3, the membrane voltage increased the sensitivity to full agonists acetylcholine (endogenous) and carbachol (artificial), but decreased the sensitivity to choline or pilocarpine, see Table S1, Fig. 3B and [59]. In support of their suggestion that voltage-sensitivity is defined by the specific binding mode of each signaling molecule to the receptor, Rinne and coworkers have shown that the replacement of Asn6.52 in the M_3 receptor by Gln reversed the voltage effect in case of the artificial agonist

carbachol but did not affect the behavior of the endogenous agonist acetylcholine [59]. The authors concluded that their data buttress the importance of the 6th helix for the mechanics of acetylcholine receptors.

Similarly, membrane voltage increased the sensitivity of dopamine D_{2S} receptor to its native agonist dopamine, but decreased the sensitivity to β-phenethylamine, *p*- and *m*-tyramine, see [69, 70] and Table S1 for further references.

By contrast, activation of the muscarinic acetylcholine receptor M_1 both by endogenous agonist acetylcholine and artificial agonist carbachol was depressed by membrane voltage, see Fig. 3C and Table S1. This behavior could be better described by the carrier-off mode, where the Na^+ ion retreats into the extracellular medium upon activation. It appears that the M_1 receptor does not translocate Na^+ even in the presence of its endogenous agonist, which may have sense if the activity of this receptor is suppressed by membrane voltage.

Finally, Table S1 also reports several cases where receptors were insensitive to membrane voltage. Mechanistically, this could happen if the displacement of the Na^+ ion - in either direction - is uncoupled from the activation (δ<<1.0). For instance, Na^+ ion could retreat before the major conformational change/activation occurs.

In summary, the suggested model allowed us to qualitatively describe the data on voltage dependence of several Na^+-dependent GPCRs by using the same set of fixed parameters for receptor activation and by varying only the affinities to the agonist and the Na^+ ion. The modeling suggests that the translocation of a Na^+ ion across the membrane and into the cytoplasm concomitantly with the receptor activation increases both the sensitivity and selectivity of GPCRs.

4.2. Structural elements of the coupling mechanism

Here we argue that the Na^+ ion serves as the physical moiety that couples the GPCR with the external electrochemical gradient by propelling, as a cannon ball, through the layer of hydrophobic residues and promoting the conformational change in the receptor. To identify the structural aspects of the coupling mechanism, we superposed crystal structures of the muscarinic acetylcholine receptor M_2 in its inactive state (PDB entry 3UON [12]) and in the active state (PDB: 4MQT [11]), see Fig. 1C. This pair of structures was chosen because of the clear-cut differences between the inactive and active structures [11, 71] and the reported voltage dependence of M_2 muscarinic receptors, see Fig. S3, [61, 62, 67, 72] and Table S1 for further references. The results of our analysis, however, should also be applicable to other Class A GPCRs because of the high sequence identity of the regions surrounding the sodium ion among the members of this class [25]. They share, for example, motifs LxxxD in helix 2, DRY in helix 3, WxP in helix 6, and NPxxY in helix 7, see Fig. 1C,D and [1, 73– 75]. Fig. 1D shows the positions of these motifs, whereas Table S2 reports the extent of their conservation.

The crystal structures of the muscarinic acetylcholine receptor M_2 in the active and inactive state differ in the conformation of helix 6 and, specifically, positions of Trp400 (6.48), Leu65 (2.46) and the residues of the NPxxY motif (Fig. 1C, residue numbers for the PDB

entry 4MQT). In the inactive state of the M_2 receptor, a large cavity above the sodium site connects it with the extracellular space, while the cytoplasmic cavity protracts only up to the residues of the NPxxY motif. As it was discussed earlier [23, 32, 36, 37, 76, 77], the connection between the two cavities is blocked by a layer of hydrophobic residues. In Fig. 1, this hydrophobic layer contains Leu65 (2.46), Leu114 (3.43), Val111(3.40), Ile117(3.46), Ile392(6.40), Leu393(6.41) and Phe396(6.44) (Fig. 1C,D). These hydrophobic residues in helices 2, 3 and 6 were previously implicated in controlling the activation-related conformational changes [23, 32, 36, 37, 76, 77]. Most of these residues are conserved in class A GPCRs (Table S2). The above-listed residues of the hydrophobic barrier are supported structurally by a second shell of conserved hydrophobic residues: Val44(1.53), Ile62(2.43), Trp148(4.50), Pro198(5.50), Met202(5.54), Tyr206(5.58), and Ile389(6.37). These residues appear to be functionally important: their positions are almost always taken by hydrophobic residues in the class A GPCRs, and in many cases not just the hydrophobic nature, but even the specific residue types are highly conserved (see Table S2).

In Fig. 1, the hydrophobic layer is centered on Leu65 (Leu2.46) of the conserved LxxxD motif. Leucines in a helix generally prefer one of two rotamers [49], and a rotamer search for Leu2.46 reveals two clearly preferred rotamers at this position (Fig. S4A). After reinterpretation of the X-ray data of the PDB entry 3UON by the PDB_REDO team [78], Leu2.46 adopts the conformation shown in Fig. 4A and S4B, which corresponds to the lower of the two preferred rotamers in Fig.S4A. The upper of the two rotamer positions is not available to Leu2.46 in the 3UON structure because the Leu side chain would clash with Asp2.50 (as shown in Fig. 4B) and Tyr7.53. Notably, in the active structure of the same receptor (PDB: 4MQT), Leu2.46 is observed in the upper rotamer, see Fig. 1C, S4C. If Leu2.46 is placed in the upper rotamer in the structure of the inactive receptor as envisioned in Fig. 4B and S4D, the two cavities get connected, indicating that water and small ions could freely traverse the GPCR helix bundle (Fig. 4). Hence, formation of a passage for a Na^+ ion requires releasing the steric hindrances by Asp2.50 and Tyr7.53, which prevent rotation of Leu2.46 into the upper rotamer position.

A minor rotameric transition of the strictly conserved Leu2.46 can open a conduit for voltage-driven translocation of Na^+ ion into the cell (Fig. 4, S4). Leu2.46 and Asp2.50 form the highly conserved motif LxxxD in helix 2, see [73] and Table 3; here Asp2.50, owing to its negative charge, is the strongest ligand of the Na^+ ion. While Asp2.50 serves as a Na^+ ligand, Leu2.46 controls the interface between helices 2 and 3. In the Na^+-translocating rhodopsin, the transmembrane ion passage is formed by helices 3, 6 and 7 [5, 38–40]; it is likely to be contributed by same helices in GPCRs [5, 23, 25, 32]. Based on the structure analysis (Fig. 4, S4), we suggest that the rotameric change of Leu2.46 upon GPCR activation plays a key role in coupling the voltage-driven Na^+ translocation into the cell with the activation of GPCRs.

Numerous alanine screening experiments, performed on different GPCRs, showed an altered function in Leu2.46 mutants, see e.g. [79]. The results of such experiments, however, are difficult to interpret. If Leu2.46 is indeed, as we suspect, involved in the coupling of GPCR activation with Na^+ translocation, then its replacement would affect both these processes with an unpredictable outcome for the function. More informative is the observation,

obtained upon alanine scanning of the human adenosine A_{2A} receptor, that the mutation of Leu2.46 to Ala (L48A) dramatically increased the thermostability of the receptor [80]. The temperature T_m at which 50% of the solubilized receptor could still bind ligand after 30 min thermo-incubation increased from 28.5°C in the wild-type protein to 42.5°C in the Leu2.46Ala mutant. The two second-best mutations increased T_m only to 34.5°C. The L48A mutation apparently fixed the human adenosine A_{2A} receptor in a (thermo)stable, active conformation [80].

Poor stability is a common property of GPCRs, which hindered their crystallization for several decades. This instability is an intrinsic property; the sensitivity of GPCRs is determined by their ability to switch between two different conformations with similar energies. Dramatic stabilization of the active conformation of A_{2A} receptor after replacing Leu2.46 by the smaller Ala indicates that the conformation of the bulky hydrophobic side chain of Leu2.46 is indeed keeping the balance between the active and inactive conformations by serving as an important "weak spot" (Bibbe and Vriend, submitted). At the same time, Leu2.46 appears to control the Na^+ path (see Fig. 4, S4), which points to this strictly conserved residue as the key coupling moiety in GPCRs.

The coupling between the electrogenic Na^+ translocation and GPCR activation would be achieved if the agonist binding decreases the affinity of GPCR for the Na^+ ion. Indeed, keeping the Na^+ ion in the middle of the hydrophobic membrane is energetically very demanding because of the high desolvation penalty for a positively charged small cation [81]. In the well-studied Na^+-dependent ATP synthases, binding of the Na^+ ion in the middle of the membrane requires six ligands [82, 83]; a loss of even one of them transforms a Na^+-translocating enzyme into a proton-translocating one [82–84]. The detachment of Na^+ from its binding site could be mediated by Trp6.48. This residue is strictly conserved in most class A GPCRs (Table S2) and changes its conformation in response to agonist binding, see Fig. 1C and [2, 7, 18–24]. Specifically, in the structure of the δ-opioid receptor (PDB: 4N6H) Trp274(6.48) interacts with the Na^+ ion via a water molecule [5, 13]; same interaction can be seen in structures of A_{2A} adenosine receptor (PDB 4EIY) and $β_1$-adrenoceptor (PDB 5A8E). In all likelihood, Trp6.48 participates in a hydrogen-bonded network also in other class A GPCRs. If the system of bonds around the Na^+ ion gets destabilized in response to the agonist binding and conformational change of Trp6.48, the further stay of the Na^+ ion in the middle of the membrane would not be possible. If the retreat path is blocked by the bound agonist, the Na^+ ion would swing in the pocket until, being pushed by electric field, it enforces the twist of Leu2.46 residue into the upper rotamer. This rotameric transition demands, however, to resolve the steric clash with Asp2.50 that is located just one helix turn away (Fig. 4B). Asp2.50 is engaged in binding of Na^+ ion and would not get aside as long as the Na^+ ion stays bound. Hence, the breakage of the bond between the Na^+ ion and Asp2.50 is a precondition of the isomeric transition of Lys2.46 and opening of the cytoplasmic Na^+ conduit (carrier-on operation mode, Fig. 2). Alternatively, the Na^+ ion could retreat, against the electric field, into the extracellular space. In this case, the electric field would prevent, rather than promote, the GPCR activation (carrier-off mode, Fig. 2). Concomitantly with the escape of the Na^+ ion, Tyr7.53 makes a new hydrogen bond, via a water bridge (with Tyr5.58 in mammals), whereas the Asn7.49 residue of the NPxxY motif turns towards Asp2.50; these changes yield a new, alternative hydrogen bond network that is seen in the

"active" crystal structures (Fig. 1B, C) [21–23]. These new hydrogen bonds prevent the return of the Na^+ ion and stabilize the active conformation of the receptor, which is accompanied by displacement of several TM helices and closing of the Na^+-binding pocket and of the cytoplasmic Na^+ path (Fig. 1B). As a result, the escape of the Na^+ ion gets thermodynamically coupled with the GPRC activation.

The suggested conformational coupling between Leu 2.46, Asp 2.50 and Tyr 7.53 is supported by very recent data of Filizola and colleagues who performed extensive steered MD simulations of the Na^+-containing μ-opioid receptor under conditions where a bias was applied to the Z coordinate of a reference sodium ion to force its movement parallel to the normal vector of the membrane surface [32]. In this system, the authors identified residue pairs whose minimum heavy atom distance fluctuations exhibited a larger than 0.6 correlation with slow most dominant time-lagged independent components of the protein fluctuation related to the Na^+ displacement. The distance fluctuations between Leu110(2.46) and Tyr336(7.53) correlated with the slowest independent component in both active and inactive states, the distance fluctuations between Asp114(2.50) and Tyr336(7.53) correlated with the slowest independent component in the inactive state. These data suggest that these residues are among molecular determinants involved in Na^+ translocation [32].

Our analysis of GPCR structures showed that the Na^+ ion might escape from the helical bundle of GPCR either after reaching the water phase from the cytoplasmic side or, even earlier, by slipping between helices 2 and 3 at the level of the DRY motif (Fig. S5). In the latter case, the Na^+ ion would be released into the layer of phosphate groups of phospholipids. Their negative charges, serving as potent alternative Na^+ ligands, could attract the Na^+ ion and help it to slide between the helices. For the Na^+ ion, in fact, there is no need to get any further. Molecular dynamics simulations of phospholipid membranes showed that Na^+ ions reside among the phosphate groups and compensate their negative charges [85].

We have observed a continuous path for the Na^+ ion only when the GPCR is in the *inactive* conformation and Leu2.46 is in the upper rotamer typical for the *active* conformation (Fig. 4, S4), which explains why the path is not seen either in the active or in inactive structures (Fig. 1, S4). Owing to the constriction by the second shell of hydrophobic resides (Table S2, Fig. 1D), the probability of a spontaneous opening of the path should be low, which might explain the relatively high activation energy of the conformational change in GPCRs [19, 32, 57, 58]. Otherwise, Na^+ ions would constantly leak through GPCRs. While the importance of Asp2.50, Trp6.48 and Tyr7.53 for activation of GPCRs and formation of a Na^+-translocating passage has been widely discussed, see e.g. [2, 21–23, 32, 36, 37], the control function of Leu2.46, to our knowledge, has not been specifically addressed until now.

4. 3. Evolutionary considerations

Earlier, the structure superposition of the Na^+-translocating rhodopsin from *Dokdonia eikasta* (NR), and Na-bound GPCRs allowed us to produce a structure-guided alignment of MRs and GPCRs and to suggest the emergence of GPCRs from Na^+ translocating MRs [5]. Here we have updated this alignment by including the wild type (not chimeric) channelrhodopsin 2, the structure of which was recently resolved [86] (ChR2, Fig. S6). As

seen in Fig. S6, the Na^+-coordinating residues of GPCRs (1.50, 2.50, 3.39, 7.45 and 7.49) correspond to the ion-coordinating residues from both NR and ChR2. The pivot Trp6.48 residue of the conserved WxP motif remains the only conserved residue between GPCRs and MRs, in agreement with the movement of the cytoplasmic half of helix 6 as the major conformational change both in MRs [87–89] and GPCRs [2, 7, 8, 19]. In addition to the previously reported similarities with NR, the updated alignment shows that Asp2.50 of GPCRs corresponds to a glutamate residue in helix 2 of ChR2, whereas the strictly conserved Trp4.50 of GPCRs is matched by a Trp residue in ChR2 (Fig. S6). The conservation patterns for functionally important residues between NR and GPCRs, on one hand, and ChR2 and GPCRs, on the other hand, overlap only partially (Fig. S6). It appears that the Na^+-translocating, MR-type ancestors of GPCRs could have combined features of NR and ChR2.

The structural similarity between GPCRs and ChR2 implies possible similarities in their mechanisms. It was shown that photoactivation of ChR was coupled not only with the motion of helix 6, but also with a rotation of helix 2 [89]. Hence, the functional mobility of helix 2, which carries the LxxxD motif, may also have been inherited from MRs.

The elements of above-described coupling machinery, including an Asp residue in the middle of the helix 2, could be seen already in representative GPCR-like proteins of early-branching eukaryotes, such as Protozoa, primitive Metazoa and plants, which are aligned in Fig. 5. Here, an Asp residue in the position that corresponds to Asp2.50 of class A GPCRs can be considered an indication of the presence of a Na^+-binding site. Otherwise, maintaining an Asp residue in the middle of the membrane would be energetically costly and this Asp would be prone to be lost in the course of evolution, as discussed below. As follows from Fig. 5, early-branching GPCR-like proteins with a counterpart of Asp2.50 often have potential Na^+ ligands also in the positions of other Na^+ ligands of class A GPCRs.

The suggested key role of Leu2.46 in controlling GPCR activation is supported not only by its already mentioned high degree of conservation within class A GPCRs (90%, see [36, 73] and Table S2), but also by its conservation within all GPCR-like proteins, even those lacking Asp2.50 (Fig. 5), which is unusual for a hydrophobic residue and indicates that the shape of the side chain of Leu2.46 is particularly important. Trp6.48, the only residue that is conserved between MRs and GPCRs (Fig. S6), is highly but not universally conserved within GPCRs: it is replaced by Tyr in some Alveolata and by Phe in the protease-activated receptor 1 (PAR1) of Metazoa. In addition to Leu2.46, hydrophobic/aromatic residues are well conserved in the positions 3.40, 3.46, 6.40 and 6.44, which correspond to the hydrophobic core of class A GPCRs, *cf.* Table S2 and Fig. 5. Residues Asn7.49 and Tyr7.53 from the NPxxY motif are all highly conserved. Finally, the characteristic motif DRY of the TM3 is absent in plants and most protozoa.

Hence, sequence comparisons of animal class A GPCRs with evolutionarily oldest, supposedly Na^+-binding, GPCR-like proteins (Fig. 5) support our suggestion on the importance of Leu2.46, Asp2.50, Trp6.48, Asn7.49, Tyr/Phe7.53 and the set of tightly packed, conserved hydrophobic residues for the function of Na^+-binding GPCRs and, specifically, for the coupling between their activation and Na^+ translocation. In contrast, the

DRY motif is absent from the sequences of GPCRs from plants and Alveolata and appears to be a somewhat later acquisition.

Our inspection showed that eukaryotic genomes contain numerous GPCR-like sequences, both with and without counterparts of Asp2.50. The latter sequences (some are shown in Fig. 5) most likely belong to GPCRs that cannot bind the Na^+ ion. Presence of other Na^+ ligands in many such sequences suggests that they could have lost their Na^+ binding capability in the course of their evolution. Loss of Na^+ binding in the course of GPCR evolution would not necessarily lead to the loss of function; the ability to shift between the active and inactive conformation in response to agonist binding could still be retained. Those residues that appear to form the mechanistic core of the coupling/activating mechanism in GPCRs are mostly conserved also in those GPCRs lacking a counterpart of Asp 2.50. Even without a bound Na^+ ion, a GPCR could be driven by voltage if its activation is coupled with proton translocation across the membrane via former Na^+ ligands. The existence of both Na^+-dependent and Na^+-independent GPCRs deserves comparison with rotary ATP synthases, which can be driven either by protons or Na^+ ions [90]. While Na^+-translocating ATP synthases are found only in some, mostly anaerobic prokaryotes [91], a comparative analysis has indicated their evolutionary primacy [82]. Apparently, in most lineages, the ability of ATP synthases to bind and translocate Na^+ ions got lost; these enzymes, however, retained less structurally demanding capacity to translocate protons, which became particularly beneficial after the oxygenation of atmosphere [92].

Although, in the absence of a Na^+-binding site, some GPCRs could still be able to harness energy of membrane voltage, such GPCRs would be unable to (i) suppress the noise by binding a Na^+ ion, (ii) exploit the concentration gradient of Na^+ ions for increasing their sensitivity and (iii) boost their selectivity by specifically amplifying the signal in response to endogenous agonists. Therefore, it is tempting to speculate that more Na^+-dependent GPCRs would be present in organisms that need particularly sensitive and selective receptors for the active exploration of their environment. Indeed, Na^+-dependent GPCRs are abundant not only in mammalian genomes, but also in genomes of primitive organisms known for their active behavior, such as free swimming, single-celled ciliates *Tetrahymena, Paramecium*, or *Stentor* (Fig. 5). For instance, the genome of *Stentor coeruleus* contains dozens of GPCR-encoding genes with a full set of Na^+ ligands.

The Ballesteros-Weinstein nomenclature [16, 17], as used in this work, attributes the index "50" to the amino acid residue that is the most conserved in each helix among class A GPCRs. Comparison of Table 3 with the multiple alignment in Fig. 5 shows that the "50th" residues, while conserved among class A GPCRs, are often not conserved within a broader set of Na^+-binding GPCRs. Proline residues 5.50, 6.50 and 7.50, which are conserved within class A GPCRs, are not conserved in receptors of primitive organisms (Fig. 5). It appears that the acquisition of additional proline residues in transmembrane helices could contribute to the success and proliferation of class A GPCRs. These proline residues could form the mechanistic scaffold of class A GPCRs, stabilize the protein fold and serve as pivots upon receptor activation. The existence of such proline scaffold would relieve the steric constrains on other residues and make class A GPCRs more prone to mutations and, hence, more evolutionarily adaptable.

Hence, Na^+-dependent GPCRs, after their emergence in primitive eukaryotes, could be fine-tuned by successive mutations to perform diverse signaling functions. Those mutations would affect their sensitivity, signal-to-noise ratio, chemical selectivity etc. Furthermore, mutations could affect even the voltage/current profiles (where current corresponds to the signal propagation) and determine whether the particular receptor would be sensitized by membrane potential (as the majority of studied GPCRs, see Fig. 3A, 3B and Table S1) or hemmed by it (such as M_1 receptor, see Fig. 3C and Table S1).

5. Conclusions

Na^+-binding GPCRs appear to be splendid molecular sensors that utilize the energy of the transmembrane sodium potential to increase their (i) sensitivity; (ii) signal-to-noise ratio, and (iii) chemical selectivity. The ability to harness external energy, in conjunction with high adaptability, might explain the presence of about 700 class A GPCR-coding genes in the human genome and should be taken into account in drug design. Further progress in the field would depend on the possibility to trace the transmembrane displacements of Na^+-ions concurrently with GPCR activation and to check how the coupling between them could be affected by specific mutations.

Supplementary Material

Refer to Web version on PubMed Central for supplementary material.

Acknowledgments:

Abbreviations

cAMP	3'−5'-cyclic adenosine monophosphate
GPCR	G-protein coupled receptor
MR	microbial rhodopsin
RMSD	root-mean-square deviation
TM	transmembrane
NR	Na-translocating microbial rhodopsin
ChR2	channelrhodopsin 2

References

[1]. Katritch V, Cherezov V, Stevens RC, Structure-function of the G protein-coupled receptor superfamily, Annu Rev Pharmacol Toxicol, 53 (2013) 531–556. [PubMed: 23140243]

[2]. Manglik A, Kim TH, Masureel M, Altenbach C, Yang Z, Hilger D, Lerch MT, Kobilka TS, Thian FS, Hubbell WL, Prosser RS, Kobilka BK, Structural insights into the dynamic process of beta2-adrenergic receptor signaling, Cell, 161 (2015) 1101–1111. [PubMed: 25981665]

[3]. Ishchenko A, Gati C, Cherezov V, Structural biology of G protein-coupled receptors: new opportunities from XFELs and cryoEM, Curr Opin Struct Biol, 51 (2018) 44–52. [PubMed: 29554543]

[4]. Nordstrom KJ, Sallman Almen M, Edstam MM, Fredriksson R, Schioth HB, Independent HHsearch, Needleman--Wunsch-based, and motif analyses reveal the overall hierarchy for most of the G protein-coupled receptor families, Molecular biology and evolution, 28 (2011) 2471–2480. [PubMed: 21402729]

[5]. Shalaeva DN, Galperin MY, Mulkidjanian AY, Eukaryotic G protein-coupled receptors as descendants of prokaryotic sodium-translocating rhodopsins, Biol. Direct, 10 (2015) 63. [PubMed: 26472483]

[6]. Palczewski K, Kumasaka T, Hori T, Behnke CA, Motoshima H, Fox BA, Le Trong I, Teller DC, Okada T, Stenkamp RE, Yamamoto M, Miyano M, Crystal structure of rhodopsin: A G protein-coupled receptor, Science, 289 (2000) 739–745. [PubMed: 10926528]

[7]. Park JH, Scheerer P, Hofmann KP, Choe HW, Ernst OP, Crystal structure of the ligand-free G-protein-coupled receptor opsin, Nature, 454 (2008) 183–187. [PubMed: 18563085]

[8]. Scheerer P, Park JH, Hildebrand PW, Kim YJ, Krauss N, Choe HW, Hofmann KP, Ernst OP, Crystal structure of opsin in its G-protein-interacting conformation, Nature, 455 (2008) 497–502. [PubMed: 18818650]

[9]. Kobilka B, Schertler GF, New G-protein-coupled receptor crystal structures: insights and limitations, Trends Pharmacol. Sci, 29 (2008) 79–83. [PubMed: 18194818]

[10]. Liu W, Chun E, Thompson AA, Chubukov P, Xu F, Katritch V, Han GW, Roth CB, Heitman LH, AP IJ, Cherezov V, Stevens RC, Structural basis for allosteric regulation of GPCRs by sodium ions, Science, 337 (2012) 232–236. [PubMed: 22798613]

[11]. Kruse AC, Ring AM, Manglik A, Hu J, Hu K, Eitel K, Hubner H, Pardon E, Valant C, Sexton PM, Christopoulos A, Felder CC, Gmeiner P, Steyaert J, Weis WI, Garcia KC, Wess J, Kobilka BK, Activation and allosteric modulation of a muscarinic acetylcholine receptor, Nature, 504 (2013) 101–106. [PubMed: 24256733]

[12]. Haga K, Kruse AC, Asada H, Yurugi-Kobayashi T, Shiroishi M, Zhang C, Weis WI, Okada T, Kobilka BK, Haga T, Kobayashi T, Structure of the human M2 muscarinic acetylcholine receptor bound to an antagonist, Nature, 482 (2012) 547–551. [PubMed: 22278061]

[13]. Fenalti G, Giguere PM, Katritch V, Huang XP, Thompson AA, Cherezov V, Roth BL, Stevens RC, Molecular control of delta-opioid receptor signalling, Nature, 506 (2014) 191–196. [PubMed: 24413399]

[14]. Miller-Gallacher JL, Nehme R, Warne T, Edwards PC, Schertler GF, Leslie AG, Tate CG, The 2.1 A resolution structure of cyanopindolol-bound beta1-adrenoceptor identifies an intramembrane Na+ ion that stabilises the ligand-free receptor, PLoS One, 9 (2014) e92727. [PubMed: 24663151]

[15]. Wacker D, Stevens RC, Roth BL, How Ligands Illuminate GPCR Molecular Pharmacology, Cell, 170 (2017) 414–427. [PubMed: 28753422]

[16]. Ballesteros JA, Weinstein H, Integrated methods for the construction of three-dimensional models and computational probing of structure-function relations in G protein-coupled receptors, in: Methods in Neurosciences, Elsevier, 1995, pp. 366–428.

[17]. Isberg V, de Graaf C, Bortolato A, Cherezov V, Katritch V, Marshall FH, Mordalski S, Pin JP, Stevens RC, Vriend G, Gloriam DE, Generic GPCR residue numbers - aligning topology maps while minding the gaps, Trends Pharmacol. Sci, 36 (2015) 22–31. [PubMed: 25541108]

[18]. Knierim B, Hofmann KP, Gartner W, Hubbell WL, Ernst OP, Rhodopsin and 9-demethyl-retinal analog: effect of a partial agonist on displacement of transmembrane helix 6 in class A G protein-coupled receptors, J. Biol. Chem, 283 (2008) 4967–4974. [PubMed: 18063586]

[19]. Knierim B, Hofmann KP, Ernst OP, Hubbell WL, Sequence of late molecular events in the activation of rhodopsin, Proc. Natl. Acad. Sci. USA, 104 (2007) 20290–20295. [PubMed: 18077356]

[20]. Shi L, Liapakis G, Xu R, Guarnieri F, Ballesteros JA, Javitch JA, Beta2 adrenergic receptor activation. Modulation of the proline kink in transmembrane 6 by a rotamer toggle switch, J Biol Chem, 277 (2002) 40989–40996. [PubMed: 12167654]

[21]. Eddy MT, Lee MY, Gao ZG, White KL, Didenko T, Horst R, Audet M, Stanczak P, McClary KM, Han GW, Jacobson KA, Stevens RC, Wuthrich K, Allosteric Coupling of Drug Binding and Intracellular Signaling in the A2A Adenosine Receptor, Cell, 172 (2018) 68–80. [PubMed: 29290469]

[22]. Yuan S, Palczewski K, Peng Q, Kolinski M, Vogel H, Filipek S, The mechanism of ligand-induced activation or inhibition of mu- and kappa-opioid receptors, Angew Chem Int Ed Engl, 54 (2015) 7560–7563. [PubMed: 25968837]

[23]. Yuan S, Hu Z, Filipek S, Vogel H, W246(6.48) opens a gate for a continuous intrinsic water pathway during activation of the adenosine A2A receptor, Angew Chem Int Ed Engl, 54 (2015) 556–559. [PubMed: 25403323]

[24]. Yuan S, Vogel H, Filipek S, The role of water and sodium ions in the activation of the mu-opioid receptor, Angew Chem Int Ed Engl, 52 (2013) 10112–10115. [PubMed: 23904331]

[25]. Katritch V, Fenalti G, Abola EE, Roth BL, Cherezov V, Stevens RC, Allosteric sodium in class A GPCR signaling, Trends Biochem. Sci, 39 (2014) 233–244. [PubMed: 24767681]

[26]. Massink A, Gutierrez-de-Teran H, Lenselink EB, Ortiz Zacarias NV, Xia L, Heitman LH, Katritch V, Stevens RC, IJzerman AP, Sodium ion binding pocket mutations and adenosine A2A receptor function, Mol. Pharmacol, 87 (2015) 305–313. [PubMed: 25473121]

[27]. White KL, Eddy MT, Gao ZG, Han GW, Lian T, Deary A, Patel N, Jacobson KA, Katritch V, Stevens RC, Structural Connection between Activation Microswitch and Allosteric Sodium Site in GPCR Signaling, Structure, 26 (2018) 259–269. [PubMed: 29395784]

[28]. Pert CB, Pasternak G, Snyder SH, Opiate agonists and antagonists discriminated by receptor binding in brain, Science, 182 (1973) 1359–1361. [PubMed: 4128222]

[29]. Horstman DA, Brandon S, Wilson AL, Guyer CA, Cragoe EJ Jr., Limbird LE, An aspartate conserved among G-protein receptors confers allosteric regulation of alpha 2-adrenergic receptors by sodium, J. Biol. Chem, 265 (1990) 21590–21595. [PubMed: 2174879]

[30]. Livingston KE, Traynor JR, Disruption of the Na+ ion binding site as a mechanism for positive allosteric modulation of the mu-opioid receptor, Proc. Natl. Acad. Sci. USA, 111 (2014) 18369–18374. [PubMed: 25489080]

[31]. Shang Y, LeRouzic V, Schneider S, Bisignano P, Pasternak GW, Filizola M, Mechanistic insights into the allosteric modulation of opioid receptors by sodium ions, Biochemistry, 53 (2014) 5140–5149. [PubMed: 25073009]

[32]. Hu X, Wang Y, Hunkele A, Provasi D, Pasternak GW, Filizola M, Kinetic and thermodynamic insights into sodium ion translocation through the mu-opioid receptor from molecular dynamics and machine learning analysis, PLoS Comput Biol, 15 (2019) e1006689. [PubMed: 30677023]

[33]. Ye L, Neale C, Sljoka A, Lyda B, Pichugin D, Tsuchimura N, Larda ST, Pomes R, Garcia AE, Ernst OP, Sunahara RK, Prosser RS, Mechanistic insights into allosteric regulation of the A2A adenosine G protein-coupled receptor by physiological cations, Nat Commun, 9 (2018) 1372. [PubMed: 29636462]

[34]. Rasmussen SG, Choi HJ, Fung JJ, Pardon E, Casarosa P, Chae PS, Devree BT, Rosenbaum DM, Thian FS, Kobilka TS, Schnapp A, Konetzki I, Sunahara RK, Gellman SH, Pautsch A, Steyaert J, Weis WI, Kobilka BK, Structure of a nanobody-stabilized active state of the beta(2) adrenoceptor, Nature, 469 (2011) 175–180. [PubMed: 21228869]

[35]. Huang W, Manglik A, Venkatakrishnan AJ, Laeremans T, Feinberg EN, Sanborn AL, Kato HE, Livingston KE, Thorsen TS, Kling RC, Granier S, Gmeiner P, Husbands SM, Traynor JR, Weis

WI, Steyaert J, Dror RO, Kobilka BK, Structural insights into micro-opioid receptor activation, Nature, 524 (2015) 315–321. [PubMed: 26245379]

[36]. Yuan S, Filipek S, Palczewski K, Vogel H, Activation of G-protein-coupled receptors correlates with the formation of a continuous internal water pathway, Nat Commun, 5 (2014) 4733. [PubMed: 25203160]

[37]. Vickery ON, Carvalheda CA, Zaidi SA, Pisliakov AV, Katritch V, Zachariae U, Intracellular Transfer of Na(+) in an Active-State G-Protein-Coupled Receptor, Structure, 26 (2018) 171–180 e172. [PubMed: 29249607]

[38]. Gushchin I, Shevchenko V, Polovinkin V, Kovalev K, Alekseev A, Round E, Borshchevskiy V, Balandin T, Popov A, Gensch T, Fahlke C, Bamann C, Willbold D, Buldt G, Bamberg E, Gordeliy V, Crystal structure of a light-driven sodium pump, Nat Struct Mol Biol, 22 (2015) 390–395. [PubMed: 25849142]

[39]. Kato HE, Inoue K, Abe-Yoshizumi R, Kato Y, Ono H, Konno M, Hososhima S, Ishizuka T, Hoque MR, Kunitomo H, Ito J, Yoshizawa S, Yamashita K, Takemoto M, Nishizawa T, Taniguchi R, Kogure K, Maturana AD, Iino Y, Yawo H, Ishitani R, Kandori H, Nureki O, Structural basis for Na(+) transport mechanism by a light-driven Na(+) pump, Nature, 521 (2015) 48–53. [PubMed: 25849775]

[40]. Kovalev K, Polovinkin V, Gushchin I, Alekseev A, Shevchenko V, Borshchevskiy V, Astashkin R, Balandin T, Bratanov D, Vaganova S, Popov A, Chupin V, Buldt G, Bamberg E, Gordeliy V, Structure and mechanisms of sodium-pumping KR2 rhodopsin, Sci Adv, 5 (2019) eaav2671. [PubMed: 30989112]

[41]. Mahaut-Smith MP, Martinez-Pinna J, Gurung IS, A role for membrane potential in regulating GPCRs?, Trends Pharmacol. Sci, 29 (2008) 421–429. [PubMed: 18621424]

[42]. Vickery ON, Machtens JP, Zachariae U, Membrane potentials regulating GPCRs: insights from experiments and molecular dynamics simulations, Curr Opin Pharmacol, 30 (2016) 44–50. [PubMed: 27474871]

[43]. MATLAB and Statistics Toolbox Release 2017a, The MathWorks, Inc, 2017.

[44]. The PyMOL Molecular Graphics System, Version 1.7.2.1, Schrödinger, LLC., 2010.

[45]. Krieger E, Vriend G, YASARA View-molecular graphics for all devices-from smartphones to workstations, Bioinformatics, 30 (2014) 2981–2982. [PubMed: 24996895]

[46]. Vriend G, WHAT IF: a molecular modeling and drug design program, J Mol Graph, 8 (1990) 52–56, 29. [PubMed: 2268628]

[47]. Voorintholt R, Kosters MT, Vegter G, Vriend G, Hol WG, A very fast program for visualizing protein surfaces, channels and cavities, J Mol Graph, 7 (1989) 243–245. [PubMed: 2486827]

[48]. Vriend G, Sander C, Detection of common three-dimensional substructures in proteins, Proteins-Structure Function and Bioinformatics, 11 (1991) 52–58.

[49]. Chinea G, Padron G, Hooft RW, Sander C, Vriend G, The use of position-specific rotamers in model building by homology, Proteins-Structure Function and Bioinformatics, 23 (1995) 415–421.

[50]. Leff P, The two-state model of receptor activation, Trends Pharmacol. Sci, 16 (1995) 89–97. [PubMed: 7540781]

[51]. Hall DA, Modeling the functional effects of allosteric modulators at pharmacological receptors: an extension of the two-state model of receptor activation, Mol Pharmacol, 58 (2000) 1412–1423. [PubMed: 11093781]

[52]. Copeland RA, The drug-target residence time model: a 10-year retrospective, Nat Rev Drug Discov, 15 (2016) 87–95. [PubMed: 26678621]

[53]. Copeland RA, Drug–target residence time, in: Keseru GM (Ed.) Thermodynamics and Kinetics of Drug Binding, Wiley-VCH Verlag GmbH, 2015, pp. 157–167.

[54]. Wikstrom M, Krab K, Saraste M, Proton-translocating cytochrome complexes, Annu Rev Biochem, 50 (1981) 623–655. [PubMed: 6267990]

[55]. Lamichhane R, Liu JJ, Pljevaljcic G, White KL, van der Schans E, Katritch V, Stevens RC, Wuthrich K, Millar DP, Single-molecule view of basal activity and activation mechanisms of the G protein-coupled receptor beta2AR, Proc Natl Acad Sci U S A, 112 (2015) 14254–14259. [PubMed: 26578769]

[56]. Ye L, Van Eps N, Zimmer M, Ernst OP, Prosser RS, Activation of the A2A adenosine G-protein-coupled receptor by conformational selection, Nature, 533 (2016) 265–268. [PubMed: 27144352]

[57]. Susac L, Eddy MT, Didenko T, Stevens RC, Wuthrich K, A2A adenosine receptor functional states characterized by (19)F-NMR, Proc Natl Acad Sci U S A, 115 (2018) 12733–12738. [PubMed: 30463958]

[58]. Arnis S, Hofmann KP, Two different forms of metarhodopsin II: Schiff base deprotonation precedes proton uptake and signaling state, Proc. Natl. Acad. Sci. USA, 90 (1993) 7849–7853. [PubMed: 8356093]

[59]. Rinne A, Mobarec JC, Mahaut-Smith M, Kolb P, Bunemann M, The mode of agonist binding to a G protein-coupled receptor switches the effect that voltage changes have on signaling, Sci Signal, 8 (2015) ra110. [PubMed: 26535008]

[60]. Rinne A, Birk A, Bunemann M, Voltage regulates adrenergic receptor function, Proc. Natl. Acad. Sci. USA, 110 (2013) 1536–1541. [PubMed: 23297214]

[61]. Ben-Chaim Y, Tour O, Dascal N, Parnas I, Parnas H, The M2 muscarinic G-protein-coupled receptor is voltage-sensitive, J. Biol. Chem, 278 (2003) 22482–22491. [PubMed: 12684524]

[62]. Ben-Chaim Y, Chanda B, Dascal N, Bezanilla F, Parnas I, Parnas H, Movement of 'gating charge' is coupled to ligand binding in a G-protein-coupled receptor, Nature, 444 (2006) 106–109. [PubMed: 17065983]

[63]. Strange PG, Agonist binding, agonist affinity and agonist efficacy at G protein-coupled receptors, Br J Pharmacol, 153 (2008) 1353–1363. [PubMed: 18223670]

[64]. Barchad-Avitzur O, Priest MF, Dekel N, Bezanilla F, Parnas H, Ben-Chaim Y, A Novel Voltage Sensor in the Orthosteric Binding Site of the M2 Muscarinic Receptor, Biophys. J, 111 (2016) 1396–1408. [PubMed: 27705763]

[65]. Mitchell P, Chemiosmotic coupling in oxidative and photosynthetic phosphorylation, Biol Rev Camb Philos Soc, 41 (1966) 445–502. [PubMed: 5329743]

[66]. Dimroth P, Bacterial energy transductions coupled to sodium ions, Res Microbiol, 141 (1990) 332–336. [PubMed: 2177912]

[67]. Navarro-Polanco RA, Moreno Galindo EG, Ferrer-Villada T, Arias M, Rigby JR, Sanchez-Chapula JA, Tristani-Firouzi M, Conformational changes in the M2 muscarinic receptor induced by membrane voltage and agonist binding, J Physiol, 589 (2011) 1741–1753. [PubMed: 21282291]

[68]. Moreno-Galindo EG, Alamilla J, Sanchez-Chapula JA, Tristani-Firouzi M, Navarro-Polanco RA, The agonist-specific voltage dependence of M2 muscarinic receptors modulates the deactivation of the acetylcholine-gated K(+) current (I KACh), Pflugers Arch, 468 (2016) 1207–1214. [PubMed: 27023349]

[69]. Sahlholm K, Marcellino D, Nilsson J, Fuxe K, Arhem P, Voltage-sensitivity at the human dopamine D2S receptor is agonist-specific, Biochem. Biophys. Res. Commun, 377 (2008) 1216–1221. [PubMed: 18983826]

[70]. Sahlholm K, Barchad-Avitzur O, Marcellino D, Gomez-Soler M, Fuxe K, Ciruela F, Arhem P, Agonist-specific voltage sensitivity at the dopamine D2S receptor--molecular determinants and relevance to therapeutic ligands, Neuropharmacology, 61 (2011) 937–949. [PubMed: 21752340]

[71]. Kruse AC, Hu J, Kobilka BK, Wess J, Muscarinic acetylcholine receptor X-ray structures: potential implications for drug development, Curr Opin Pharmacol, 16 (2014) 24–30. [PubMed: 24662799]

[72]. Ben Chaim Y, Bochnik S, Parnas I, Parnas H, Voltage affects the dissociation rate constant of the m2 muscarinic receptor, PLoS One, 8 (2013) e74354. [PubMed: 24019965]

[73]. Oliveira L, Paiva A.C.d.M., Vriend G, A common motif in G-protein-coupled seven transmembrane helix receptors, J Comput Aid Mol Des, 7 (1993) 649–658.

[74]. Nygaard R, Frimurer TM, Holst B, Rosenkilde MM, Schwartz TW, Ligand binding and micro-switches in 7TM receptor structures, Trends Pharmacol. Sci, 30 (2009) 249–259. [PubMed: 19375807]

[75]. Trzaskowski B, Latek D, Yuan S, Ghoshdastider U, Debinski A, Filipek S, Action of molecular switches in GPCRs--theoretical and experimental studies, Curr Med Chem, 19 (2012) 1090–1109. [PubMed: 22300046]

[76]. Okada T, Ernst OP, Palczewski K, Hofmann KP, Activation of rhodopsin: new insights from structural and biochemical studies, Trends Biochem. Sci, 26 (2001) 318–324. [PubMed: 11343925]

[77]. Tehan BG, Bortolato A, Blaney FE, Weir MP, Mason JS, Unifying family A GPCR theories of activation, Pharmacol Ther, 143 (2014) 51–60. [PubMed: 24561131]

[78]. Joosten RP, Long F, Murshudov GN, Perrakis A, The PDB_REDO server for macromolecular structure model optimization, IUCrJ, 1 (2014) 213–220.

[79]. Bee MS, Hulme EC, Functional analysis of transmembrane domain 2 of the M1 muscarinic acetylcholine receptor, J. Biol. Chem, 282 (2007) 32471–32479. [PubMed: 17823120]

[80]. Lebon G, Warne T, Edwards PC, Bennett K, Langmead CJ, Leslie AGW, Tate CG, Agonist-bound adenosine A(2A) receptor structures reveal common features of GPCR activation, Nature, 474 (2011) 521–525. [PubMed: 21593763]

[81]. Warshel A, Russell ST, Calculations of electrostatic interactions in biological systems and in solutions, Q Rev Biophys, 17 (1984) 283–422. [PubMed: 6098916]

[82]. Mulkidjanian AY, Galperin MY, Makarova KS, Wolf YI, Koonin EV, Evolutionary primacy of sodium bioenergetics, Biol. Direct, 3 (2008) 13. [PubMed: 18380897]

[83]. Meier T, Krah A, Bond PJ, Pogoryelov D, Diederichs K, Faraldo-Gomez JD, Complete ion-coordination structure in the rotor ring of Na+-dependent F-ATP synthases, J. Mol. Biol, 391 (2009) 498–507. [PubMed: 19500592]

[84]. Kaim G, Wehrle F, Gerike U, Dimroth P, Molecular basis for the coupling ion selectivity of F1F0 ATP synthases: probing the liganding groups for Na+ and Li+ in the c subunit of the ATP synthase from Propionigenium modestum, Biochemistry, 36 (1997) 9185–9194. [PubMed: 9230051]

[85]. Dickey A, Faller R, Examining the contributions of lipid shape and headgroup charge on bilayer behavior, Biophys. J, 95 (2008) 2636–2646. [PubMed: 18515396]

[86]. Volkov O, Kovalev K, Polovinkin V, Borshchevskiy V, Bamann C, Astashkin R, Marin E, Popov A, Balandin T, Willbold D, Buldt G, Bamberg E, Gordeliy V, Structural insights into ion conduction by channelrhodopsin 2, Science, 358 (2017) eaan8862. [PubMed: 29170206]

[87]. Wegener AA, Chizhov I, Engelhard M, Steinhoff HJ, Time-resolved detection of transient movement of helix F in spin-labelled pharaonis sensory rhodopsin II, J. Mol. Biol, 301 (2000) 881–891. [PubMed: 10966793]

[88]. Klare JP, Bordignon E, Engelhard M, Steinhoff HJ, Sensory rhodopsin II and bacteriorhodopsin: light activated helix F movement, Photochem. Photobiol. Sci, 3 (2004) 543–547. [PubMed: 15170483]

[89]. Sattig T, Rickert C, Bamberg E, Steinhoff HJ, Bamann C, Light-induced movement of the transmembrane helix B in channelrhodopsin-2, Angew Chem Int Ed Engl, 52 (2013) 9705–9708. [PubMed: 23893661]

[90]. Dimroth P, von Ballmoos C, Meier T, Catalytic and mechanical cycles in F-ATP synthases. Fourth in the Cycles Review Series, EMBO Rep, 7 (2006) 276–282. [PubMed: 16607397]

[91]. Mulkidjanian AY, Dibrov P, Galperin MY, The past and present of sodium energetics: may the sodium-motive force be with you, Biochim. Biophys. Acta, 1777 (2008) 985–992. [PubMed: 18485887]

[92]. Dibrova DV, Galperin MY, Koonin EV, Mulkidjanian AY, Ancient systems of sodium/potassium homeostasis as predecessors of membrane bioenergetics, Biochemistry (Mosc), 80 (2015) 495–516. [PubMed: 26071768]
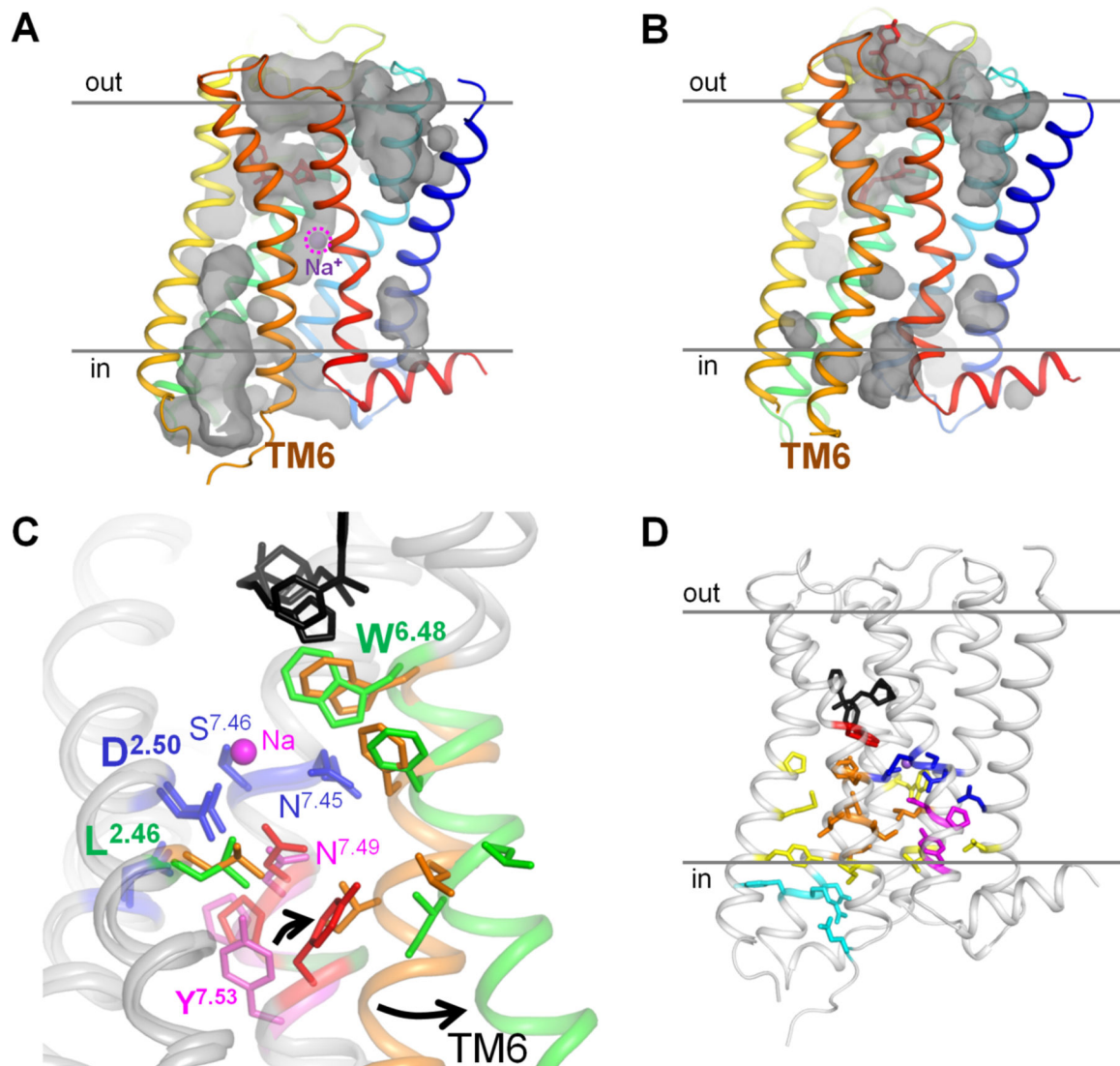
Author Manuscript

Author Manuscript

Author Manuscript

Author Manuscript

Figure 1. Active and inactive conformations of GPCRs.
A, B, conformations of the muscarinic acetylcholine receptor M_2 in the inactive state (A, PDB 3UON [12]) and active state (B, PDB 4MQT [11]) with cavities shown; "out" indicates the extracellular side, "in" indicates the cytoplasmic side. **C**. Superposition of the structures of M_2 receptor in the inactive state (the first layer of hydrophobic residues around the Na^+-binding site colored ochre and residues of the NPxxY motif colored magenta) and in the active state (the first layer of hydrophobic residues around the Na^+-binding site colored green and residues of the NPxxY motif colored red). The protein is shown as a gray cartoon, the agonist LY2119620 and antagonist 3-quinuclidinyl-benzilate are in black, Na^+-coordinating residues are colored dark blue. **D**, Overall distribution of conserved motifs and hydrophobic residue clusters in the M_2 receptor (inactive state, PDB 3UON). The Trp6.48 residue is colored red, the second layer of hydrophobic residues is colored yellow, the residues of the DRY motif and the ionic lock are in light blue. Otherwise the color code as on panel C.
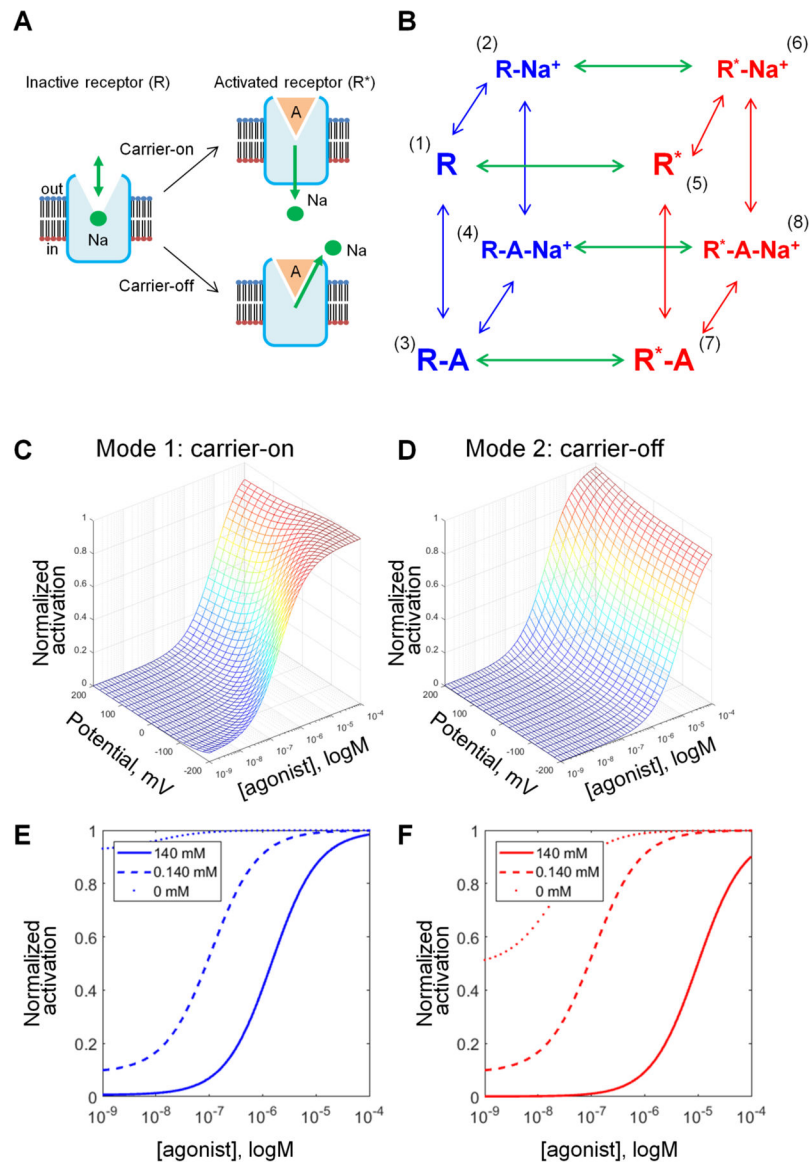
Figure 2. Kinetic models describing the behavior of the Na$^+$ ion upon GPCR activation.
A, Schematic representation of GPCR activation in carrier-on and carrier-off modes. In both modes, the Na$^+$ ion has an affinity to the inactive state of a GPCR, but not to its active state. When activation of the receptor is triggered by the agonist binding, Na$^+$ leaves its binding site. In mode 1 (carrier-on), Na$^+$ escapes to the cytoplasm, thus penetrating the membrane. In mode 2 (carrier-off), the Na$^+$ ion escapes back into the extracellular space. **B,** General scheme of the model that describes the effects of the agonist and Na$^+$ as allosteric modulators on the distribution of the receptor between the inactive states (R, shown in blue) and active states (R*, shown in red). Transitions between active and inactive states are shown as green arrows, probability coefficients are given without components describing the influence of the electrochemical gradient, which are different for "carrier-on" and "carrier-off" modes. Transition probabilities are defined in Table 1. **C, D,** Effects of the membrane potential on the concentration-response curves of GPCR activation as calculated for the

mode 1 (carrier-on) (C) and mode 2 (carrier-off) (D). The curves were plotted with constant allosteric coefficients ($\alpha, \beta, \gamma, \delta$) from Table 2, $M=10^5$, $N=10^5$, and $\theta=0.65$; **E, F**, Effects of $[Na^+]_{out}$ on the concentration-response curves of GPCR activation, the membrane voltage was set to −90 mV, other parameters as in Table 2.
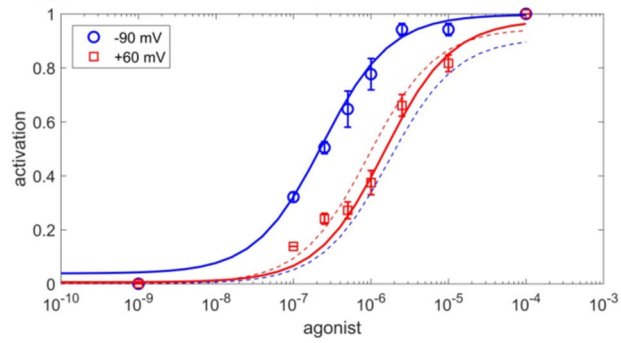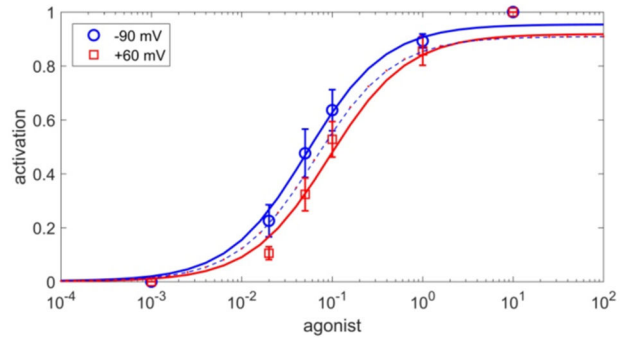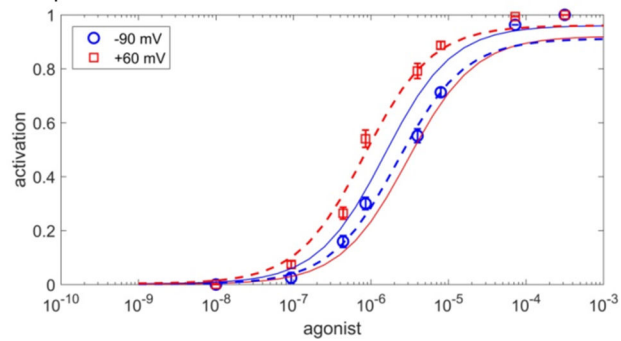
Figure 3. Fitting experimental data of voltage-sensitive GPCR activation.

The fits for the carrier-on mode 1 are shown by solid lines, the fits for the carrier-off mode 2 are shown by dashed lines. **A.** α_{2A} adrenoreceptor (α_{2A}AR) activation by the full endogenous agonist norepinephrine, experimental data from [60]. **B.** Muscarinic M_3 receptor (M_3R) activation by full agonist carbachol, experimental data from [59]. **C.** Muscarinic M_1 receptor (M_1R) activation by the full agonist carbachol, experimental data from [59].
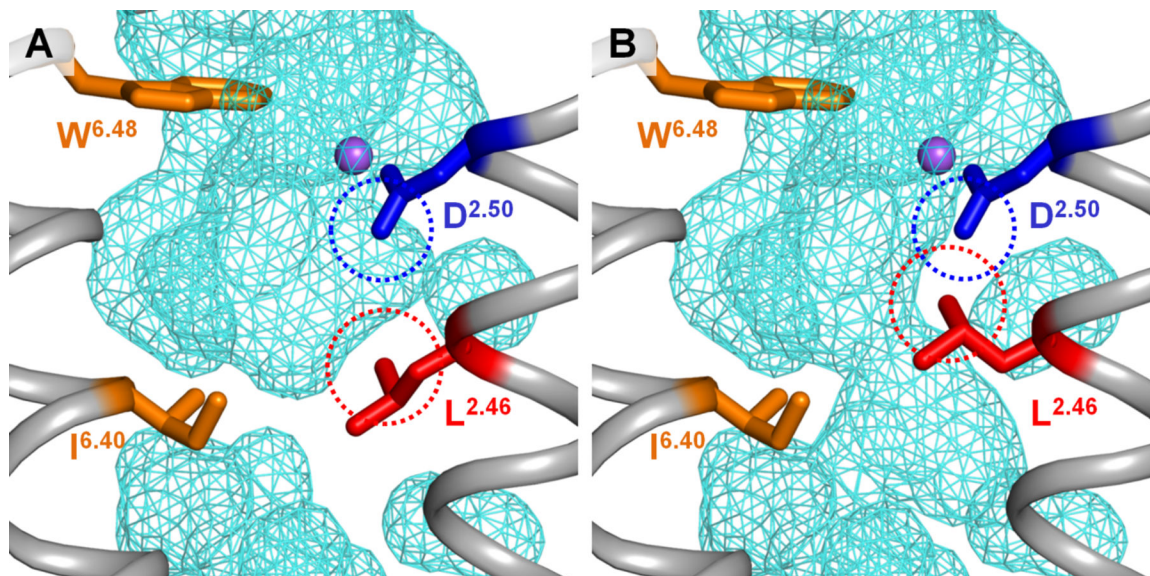
Figure 4. Conformation of Leu2.46 affects the suggested pathway of Na$^+$ escape to the cytoplasm in the muscarinic acetylcholine receptor M$_2$.

A. Sodium-binding cavity in the M$_2$ receptor in the antagonist-bound inactive state (PDB 3UON, [12]). **B**. A minor rotameric transition of Leu2.46 alone is enough to open the connection between two inner cavities, allowing the Na$^+$ ion passage through the layer of conserved hydrophobic residues (see also Fig. S4). The dashed circles mark the Van der Waals radii as calculated by the PyMol v 1.7 software [44].
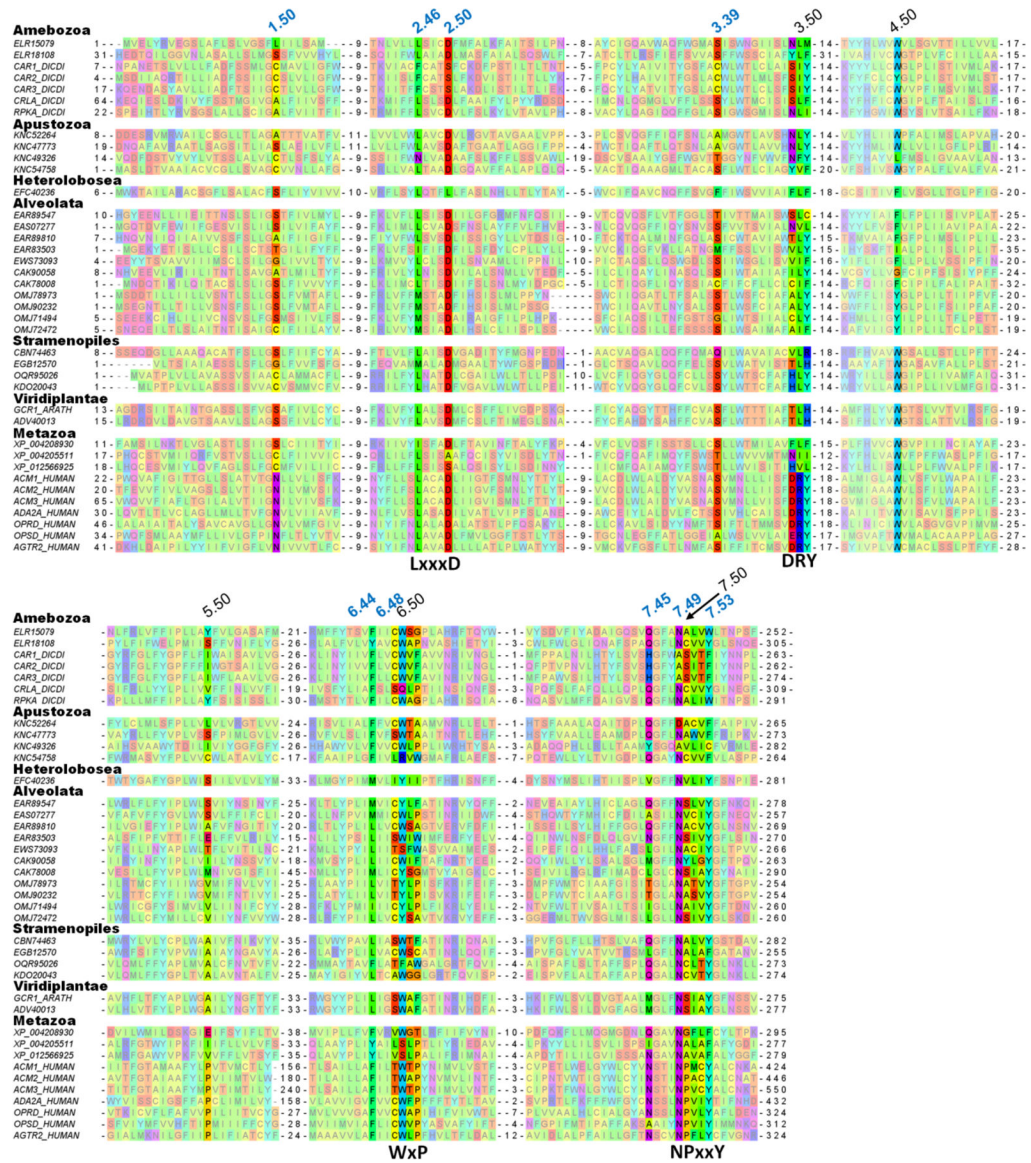
Figure 5. Multiple sequence alignment of class A GPCRs from primitive organisms.
The numbering of residues potentially involved in Na+ coordination is in blue, the numbers of the most conserved residues in each helix are in black. Sequences are listed under their GenBank, UniProt or RefSeq accession numbers, the full list of protein names and organisms is available in Fig. S7 in Supplementary Materials.

Table 1.

Equilibrium probability coefficients for the model of GPCR activation

Receptor state	Notation	Relative probabilities	
		carrier-on mode	**carrier-off mode**
Inactive	1	1	1
Inactive with a Na^+ ion	2	$\Phi_1 \cdot M[Na]^{out}$	$\Phi_1 \cdot M[Na]^{out}$
Inactive with an agonist	3	$N \cdot [A]$	$N \cdot [A]$
Inactive with an agonist and a Na^+ ion	4	$\gamma \cdot N[A] \cdot \Phi_1 \cdot M[Na]^{out}$	$\gamma \cdot N[A] \cdot \Phi_1 \cdot M[Na]^{out}$
Active	5	L	L
Active with a Na^+ ion	6	$\alpha \cdot L \cdot \Phi_2 \cdot M[Na]^{in}$	$\alpha \cdot L \cdot \Phi_1 \cdot M[Na]^{out}$
Active with an agonist	7	$\beta \cdot L \cdot N[A]$	$\beta \cdot L \cdot N[A]$
Active with an agonist and a Na^+ ion	8	$\delta(\gamma(L \cdot \beta N[A] \cdot \alpha \Phi_2 M[Na]^{in})) = \alpha\beta\gamma\delta \cdot L \cdot N[A] \cdot \Phi_2 M[Na]^{in}$	$\delta(\gamma(L \cdot \beta N[A] \cdot \alpha \Phi_1 M[Na]^{out})) = \alpha\beta\gamma\delta \cdot L \cdot N[A] \cdot \Phi_1 M[Na]^{out}$

Table 2.

Initial parameters of the model

Parameter	Value	Description[a]
M	10^3 M^{-1}	Association constant of the sodium ion (initial value)
N	10^7 M^{-1}	Association constant of the agonist (initial value)
L	1	Receptor activation constant
α	10^{-3}	Intrinsic efficacy of sodium: ratio of affinity of sodium for R* and R
β	10^3	Intrinsic efficacy of the agonist: ratio of affinity of the agonist for R* and R
γ	10^{-2}	Binding cooperativity between the sodium ion and the agonist: ratio of affinity of A for R-Na and R, or of Na for R-A and R
δ	10^2	Activation cooperativity between the sodium ion and the agonist: ratio of affinity of A for R*-Na and R-Na, or of Na for R*-A and R-A
[Na$^+$]$_{out}$	140 mM	[Na$^+$] in the extracellular medium
[Na$^+$]$_{in}$	10 mM	[Na$^+$] in the cell cytoplasm

[a]The designations of parameters are taken from ref. [51].

Table 3.

Sodium ion and agonist binding constants as obtained from fitting experimental data

Receptor – agonist pairing	Mode	β=1000		β=100	
		Na$^+$ association constant, M^{-1}	Agonist association constant, M^{-1}	Na$^+$ association constant, M^{-1}	Agonist association constant, M^{-1}
α$_{2A}$-AR with norepinephrine	1, carrier-on	2.4×10^4	2.6×10^5	8.7×10^3	1.1×10^6
M$_3$ muscarinic receptor with carbachol	1, carrier-on	3.5×10^5	8.4	3.1×10^5	87.9
M$_1$ muscarinic receptor with carbachol	2, carrier-off	2.1×10^7	6.4×10^5	2.2×10^5	2.6×10^6